Effect of dynamic and static friction on an asymmetric granular piston

Julian Talbot* and Pascal Viot†

Laboratoire de Physique Théorique de la Matière Condensée, UPMC, CNRS UMR 7600, 4, place Jussieu, 75252 Paris Cedex 05, France

(Received 14 October 2011; revised manuscript received 29 December 2011; published 29 February 2012)

We investigate the influence of dry friction on an asymmetric, granular piston of mass M, composed of two materials, undergoing inelastic collisions with bath particles of mass m. Numerical simulations of the Boltzmann-Lorentz equation reveal the existence of two scaling regimes depending on the friction strength. In the large friction limit, we introduce an exact model giving the asymptotic behavior of the Boltzmann-Lorentz equation. For small friction and for large mass ratio M/m, we derive a Fokker-Planck equation for which the exact solution is also obtained. Static friction attenuates the motor effect and results in a discontinuous velocity distribution.

DOI: 10.1103/PhysRevE.85.021310 PACS number(s): 45.70.Vn, 05.10.Gg

I. INTRODUCTION

An adiabatic piston separating two compartments of gases is a widely studied model in statistical physics. The initial interest arose from the observation that the equilibrium state cannot be predicted by application of the first and second laws of thermodynamics [1–5]. It was shown that dynamics contains different time scales before the system reaches equilibrium (for finite-size compartments) or a steady state where the piston acquires a nonzero drift velocity (for infinite compartments) [6].

The granular version of the system, where the gas particles undergo dissipative collisions, also displays interesting behavior. Brito *et al*. [7] showed that the piston eventually collapses to one side and Brey and Khalil [8] showed that the steady state is characterized by equal cooling rates in the two compartments.

The model was investigated in the context of a granular motor by Costantini *et al*. [9]. They considered a piston composed of two different materials and showed that fluctuations on the right and left sides result in noise rectification that can be converted into mechanical work. When the bath density is low, the appropriate kinetic description of the system is the Boltzmann-Lorentz equation. However, an exact solution cannot be obtained even for this simple model. Costantini *et al*. [10] proposed an ansatz of the velocity distribution, where parameters are obtained by calculating successive moments of the kinetic equation. Comparisons with numerical simulations showed that the approach is reasonable, but it fails in the limit of large piston mass (the Brownian limit). Talbot *et al*. [11] introduced a mechanical treatment that gives an exact expression for the drift velocity in the Brownian limit.

Recently, Eshuis *et al*. [12] presented the first experimental realization of a macroscopic, rotational ratchet in a granular gas. The device, which consists of four vanes, is reminiscent of that imagined by Smoluchowski [13,14]. When a soft coating was applied to one side of each vane, a motor effect was observed above a critical granular temperature. While this was the first experimental realization of a granular motor, similar Brownian ratchets exist in many diverse applications, e.g., photovoltaic devices and biological motors; see [15–17]. All of these motors share the common features of nonequilibrium conditions and spatial symmetry breaking. Several recent theoretical studies of idealized models of granular motors, which use a Boltzmann-Lorentz description [10,11,18–20], confirm that the motor effect is particularly pronounced when the device is constructed from two different materials, as was the case in the recent experiment [12]. The existing theories, however, predict a motor effect for any temperature of the granular gas while in the experiment the phenomenon is observed only if the bath temperature is sufficiently large.

Friction likely plays an important role in the experiment [12] as it does in other systems with stochastic dynamics [21–24]. Theoretical studies addressing the effect of dry (Coulombic) friction on Brownian motion were pioneered by Caughey and co-workers [25,26] and later by de Gennes [27] and Hayakawa [28]. Subsequently, Kawarada and Hayakawa [29] showed that the signature of Coulombic friction is an exponentially decaying velocity distribution function. Menzel and Goldenfeld [30] studied a Fokker-Planck equation and noted a formal connection to the Schrödinger equation for the quantum mechanical oscillator with a δ potential. Mauger [31] showed that Coulomb friction is responsible for an exponential decay of the velocity distribution when dynamics is described by a Fokker-Planck equation. Touchette and co-workers [32–34] obtained a solution of a model with dry friction and viscous damping. Experimental studies have examined droplets on nonwettable surfaces subjected to an asymmetric lateral vibration [35], as well as the biased motion of a water drop on a tilted surface subject to vibration [22,23,36].

Recently, we used numerical simulation and kinetic theory to examine the effect of dynamic friction on a chiral rotor within the framework of the Boltzmann-Lorentz equation [37]. The numerical simulations revealed the existence of two scaling regimes at low and high bath temperatures. For large rotor masses and small friction the model can be mapped onto a Fokker-Planck equation that can be solved analytically. We also obtained analytic solutions for the mean angular velocity and the angular velocity distribution function in the limit of large friction. The purpose of the present paper is to present a complete analysis of the effect of dynamic and static friction on the asymmetric granular piston.

In Sec. II, we introduce the model of a granular piston with friction. We perform numerical simulations of the Boltzmann-Lorentz (BL) equation in Sec. III. A time scale analysis

*talbot@lptmc.jussieu.fr
†viot@lptmc.jussieu.fr

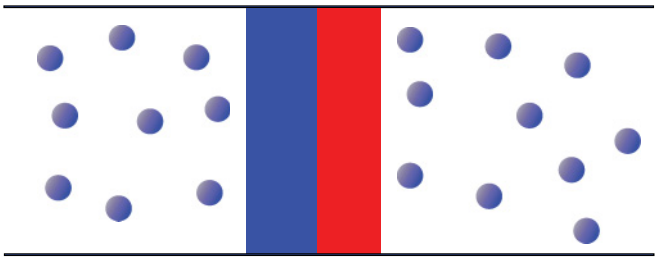

FIG. 1. (Color online) The asymmetric granular piston in a bath of thermalized particles.

presented in Sec. IV suggests that the model can be solved in two limiting cases. In Sec. V, we first consider the high friction limit by introducing the independent kick model and compare the exact solution of the model with numerical simulations of the BL equation. In the Brownian limit and in the small friction limit, we show that the Fokker-Planck equation, for which analytical solutions can be obtained, provides an accurate description of the BL equation. In Sec. VII, we generalize our study by including the effect of static friction and we briefly conclude in Sec. VIII.

II. THE MODEL

An infinite cylinder filled with a monodisperse gas composed of particles of mass m is separated into two compartments by a granular piston of mass M and of a cross-sectional area S that is composed of two materials characterized by the coefficients of restitution α_+ and α_-; see Fig. 1. The piston is constrained to move along the symmetric axis of the container and undergoes collisions with the gas particles. In addition, a frictional force of constant strength F, which acts to oppose the motion of the piston, is present. In the absence of the bath particles the equation of motion of the piston is

$$M\frac{dV}{dt} = -\sigma(V)F, \tag{1}$$

where V is the piston velocity and

$$\sigma(V) = \begin{cases} +1 & \text{if} \quad V > 0, \\ 0 & \text{if} \quad V = 0, \\ -1 & \text{if} \quad V < 0. \end{cases} \tag{2}$$

Due to the translational invariance along the perpendicular axis of the container and assuming that the cross-sectional area S of the cylinder is sufficiently large, boundary effects can be neglected. Consequently, the collision rules involve only the velocity component along the the cylinder axis. If v is the precollisional velocity of the bath particle, the postcollisional velocities of the piston and gas particles are

$$V'_{\alpha_\pm} = V + \frac{1+\alpha_\pm}{1+\mu}(v - V), \tag{3}$$

$$v'_{\alpha_\pm} = v - \frac{\mu(1+\alpha_\pm)}{1+\mu}(v - V), \tag{4}$$

where $\mu = \frac{M}{m}$ is the mass ratio and α_+ (α_-) is selected if the collision occurs on the left (right) hand side of the piston, i.e., if $v - V > 0$ ($v - V < 0$).

Precollisional (or restituting) velocities $V''_{\alpha_\pm}, v''_{\alpha_\pm}$ can be obtained from Eqs. (3) and (4) by replacing $\alpha_\pm$ with $\alpha_\pm^{-1}$.

The kinetic properties of the piston are described by means of the Boltzmann-Lorentz equation. Let us denote by $f(V;t)$ the probability density of finding the piston moving with velocity V and let $\phi(v)$ represent the velocity distribution of the bath particles at time t; then one has

$$\frac{\partial}{\partial t}f(V;t) - F\frac{\sigma(V)}{M}\frac{\partial}{\partial V}f(V;t) = J[\phi, f], \tag{5}$$

where $J[\phi, f]$ is the collision operator expressed as

$$J[f,\phi] = \rho\int_{-\infty}^{\infty} dv\,|v - V|\left[\theta(v - V)\frac{f(V''_{\alpha_+};t)}{\alpha_+^2}\phi(v'') + \theta(V - v)\frac{f(V''_{\alpha_-};t)}{\alpha_-^2}\phi(v'')\right] - \rho\nu(V)f(V;t), \tag{6}$$

where the bath density per unit length is $\rho = Sn$, n being the number density of bath particles and the Heaviside function. (Note that the model can also describe a two-dimensional system. Due to the translational invariance in the direction perpendicular to the horizontal axis, the Boltzmann-Lorentz equation is unchanged, but $\rho = Ln$ where n is then the two-dimensional density and L is the vertical length of the piston.)

$$\rho\nu(V) = \rho\int_{-\infty}^{\infty} dv|v - V|\phi(v) \tag{7}$$

is the collision rate of bath particles with (both sides of) the piston moving with a velocity V. Note that the Boltzmann-Lorentz equation neglects recollisions. This assumption is valid if the bath density ρ is low and when the mass of the piston is larger than the mass of bath particles. We note that temperature gradients are typically present in experiments [38,39] (but can be minimized or eliminated in quasi-two-dimensional systems [40,41]). They can, in principle, be included in the Boltzmann-Lorentz description, but we neglect them here for the sake of simplicity. Finally, the bath distribution $\phi(v)$ is assumed stationary and symmetric such that $\langle v\rangle = 0$.

By using appropriate changes of variables [42], the kinetic equation can be rewritten as

$$\frac{1}{\rho}\frac{\partial}{\partial t}f(V;t) - \frac{F\sigma(V)}{M\rho}\frac{\partial}{\partial V}f(V;t) = \int_0^\infty dy\,y\left[f\left(V - \frac{1+\alpha_+}{1+\mu}y;t\right)\phi\left(V + \frac{\mu-\alpha_+}{1+\mu}y\right) + f\left(V + \frac{1+\alpha_-}{1+\mu}y;t\right)\times\phi\left(V - \frac{\mu-\alpha_-}{1+\mu}y\right)\right] - f(V;t)\int_0^\infty dy\,y[\phi(V+y) + \phi(V-y)]. \tag{8}$$

It is convenient to introduce the reduced variables $F^* = F/(\rho T)$ and $V^* = \sqrt{m/T}V$, where T denotes the granular temperature of the bath particles. With this choice the average drift velocity depends only on F^*, M/m, and $\alpha_\pm$. In an experiment, the frictional force depends on the physical properties of the motor and is not easily changed. On the other hand, the granular temperature of the bath particles may be varied by increasing or decreasing the vibration amplitude or frequency of the mechanical shaker driving the granular gas particles. The relationship is not simple, however, due to the presence of temperature gradients in the experiments.

Where possible we give analytic results for a general bath particle velocity distribution, $\phi(v)$. For illustrative purposes, as well as to test the theory by comparison with numerical simulation of the BL equation, we will use a Gaussian distribution:

$$\phi(v) = \sqrt{\frac{m}{2\pi T}} \exp\left(-\frac{mv^2}{2T}\right). \tag{9}$$

III. NUMERICAL SIMULATION

We performed numerical simulations of the Boltzmann-Lorentz equation using the Gillespie method [43] for different mass ratios and for a large range of dry friction. The Gillespie method is equivalent to the Direct Simulation Monte Carlo (DSMC) method [44–47]; both provide stochastic solutions of the Boltzmann-Lorentz equation. The Gillespie algorithm generates collision events separated by exponentially distributed waiting intervals. Specifically, the probability that no event (collision) occurs in the time interval $(0, \Delta t)$ is given by

$$P(\Delta t) = \exp\left(-\rho \int_0^{\Delta t} v(t')dt'\right). \tag{10}$$

In the present application the mean collision flux $\rho v(t)$ is time dependent as the piston decelerates between collisions. A collision time Δt is generated by solving (numerically) the implicit equation

$$\ln(\xi) = -\rho \int_0^{\Delta t} v(t')dt', \tag{11}$$

where $0 < \xi < 1$ is a uniformly distributed random number. The system time is incremented by Δt and the collision is performed by sampling a velocity of the colliding bath particle using the imposed velocity distribution $\phi(v)$ and updating the piston's velocity using the collision rule Eq. (3). Full details can be found in Ref. [43].

Figure 2 shows a log-log plot of the mean velocity $\langle V^* \rangle$ of an asymmetric piston ($\alpha_+ = 1$, $\alpha_- = 0$) as a function of the dimensionless dry friction F^* for different mass ratios $\mu = 1,2,5,10,20$. We observe two scaling regimes: at low dimensionless friction force F^* the dimensionless mean velocity depends weakly on F^*, whereas in the high friction limit $F^* > 1$, $\langle V^* \rangle$ decays as F^{*-1}.

Useful insight can be obtained by observing the dynamics for different values of F^*; see Fig. 3. For $F^* = 1.0$ the motor decelerates rapidly after each collision until it comes to rest. It remains motionless until it is struck by another bath particle. For the smallest value $F^* = 0.01$, the deceleration is weak and the piston is always in motion. $F^* = 0.1$ is an intermediate case.

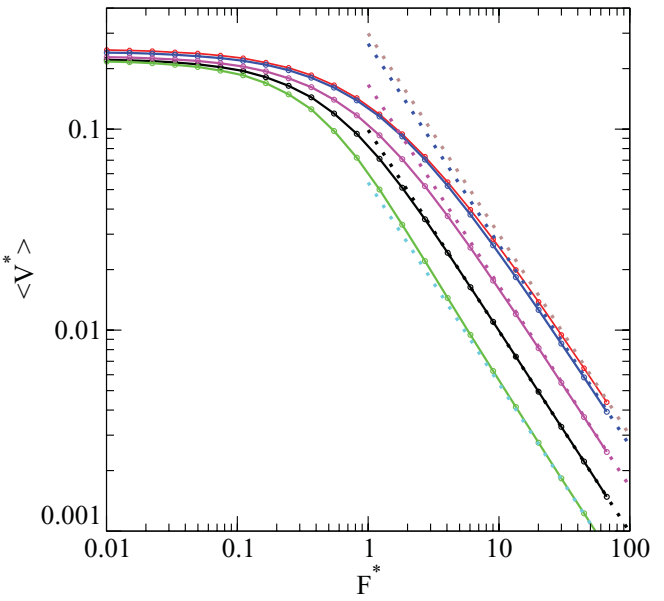

FIG. 2. (Color online) Log-log plot of the dimensionless mean velocity $\langle V^* \rangle$ of an asymmetric granular piston versus the dimensionless friction force F^* with $\alpha_+ = 1$ and $\alpha_- = 0$, for different mass ratios $\mu = 1,2,5,10,20$, top to bottom. The dotted curves correspond to the analytical expression of the large friction model and the solid curves show simulation results.

We have also monitored the ratio R of the number of collisions occurring when the piston is at rest to the total number collisions. Figure 4 shows R as a function of F^* for $M/m = 1,2,10,20$. As R approaches 1 the dynamics consists

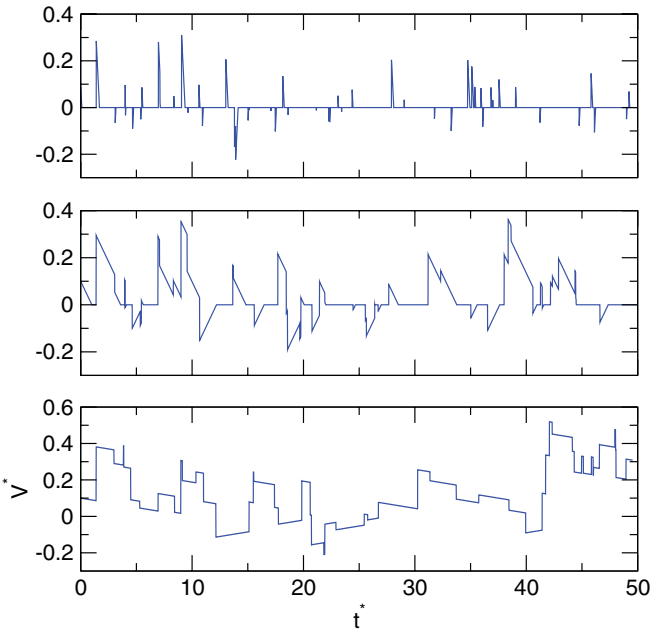

FIG. 3. (Color online) The dimensionless velocity V^* as a function of the reduced time $t^* = \rho v(0)t$ obtained from stochastic simulations of the Boltzmann-Lorentz equation. $F^* = 1.0,0.1,0.01$ from top to bottom. $\mu = 10$.

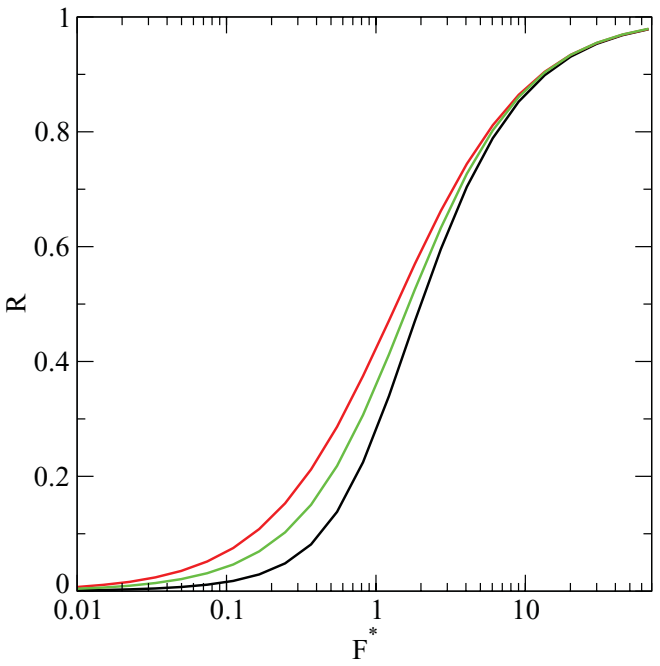

FIG. 4. (Color online) Fraction of collisions occurring when the piston is at rest over the number of collisions for different masses from numerical simulations. From left to right, $\mu = 2,5,20$.

of a series of independent displacements, each followed by a period of rest before the next collision with a bath particle.

IV. TIME SCALE ANALYSIS

As we will show, the behavior of the system is governed by the relative values of the mean collision time and the mean stopping time. The mean intercollision time between bath particles and the piston,

$$\tau_c \simeq \frac{1}{\rho \nu(0)}, \tag{12}$$

is $\tau_c \simeq \sqrt{\frac{\pi m}{2T}}\frac{1}{\rho}$ for a Gaussian bath distribution, and the mean stopping time with friction present is $\tau_s = \frac{M\overline{V}}{F}$, where $\overline{V}$ is the average velocity after a collision. When the dimensionless friction F^* is small, $\overline{V^*} \sim (\alpha_+ - \alpha_-)$, while for $F^* \gg 1$, $\overline{V^*} \sim \frac{m}{M}(\alpha_+ - \alpha_-)$, which gives

$$\frac{\tau_s}{\tau_c} \sim \frac{\alpha_+ - \alpha_-}{F^*} \times \begin{cases} 1, & F^* \gg 1, \\ \mu, & F^* \ll 1. \end{cases} \tag{13}$$

This behavior is illustrated in Fig. 3, where one observes that $\tau_s \ll \tau_c$ for $F^* = 1$, whereas $\tau_s \gg \tau_c$ for $F^* = 0.01$.

Whenever the dynamics consists of successive slip-stick motions, the velocity distribution function of the piston contains a regular part and a δ singularity at $V^* = 0$ corresponding to the situation where the piston is at rest for a finite time before the next collision with a bath particle:

$$f(V^*) = \gamma f_R(V^*) + (1-\gamma)\delta(V^*). \tag{14}$$

Here $f_R(V^*)$ is the regular part, $\int dV^* f_R(V^*) = 1$, and γ is a constant that can be determined from conservation of the probability current (for simplicity we do not use the star notation for the reduced distribution functions) at $V^* = 0$ [32]:

$$(1-\gamma)\int_{-\infty}^{\infty} dv^* |v^*| \phi(v^*) = 2\gamma f_R(0)\frac{F^*}{\mu}, \tag{15}$$

where $v^* = v\sqrt{m/T}$, which gives

$$\gamma^{-1} = 1 + 2C\frac{F^*}{\mu} \tag{16}$$

with $C = 2f_R(0)/\int_{-\infty}^{\infty} dy|y|\phi(y)$ a numerical constant.

When $\tau_c \gg \tau_s$ the frictional force stops the piston before the next collision, and the motor essentially evolves by following a sequence of stick-slip motions. Most of the time, the piston is at rest and the singular contribution is dominant, $\gamma \simeq 1/F^*$. This regime can be described by the independent kick model introduced below.

Conversely, when $\tau_c \ll \tau_s$, collisions are so frequent that sliding dominates the piston dynamics. For all practical purposes, the piston never stops or stops for an infinitesimal duration and $(1-\gamma) \simeq F^*$. In this case, the dynamics is well described by a Fokker-Planck equation for $M/m \gg 1$.

V. INDEPENDENT KICK MODEL

When the friction force is large, the stopping time τ_s is much shorter than the mean time between collisions, τ_c. The piston dynamics is then a sequence of uncorrelated kicks immediately followed by a decelerated motion that is stopped before the next collision with a particle bath. (For a more rigorous derivation of this model from the Boltzmann-Lorentz equation, see the Appendix.) The mean velocity is the average over all collisions:

$$\langle V \rangle = \rho \int_{-\infty}^{\infty} dv |v| \phi(v) \int_0^{\tau} V(t) dt, \tag{17}$$

where $V(t) = V_0 - \frac{F\sigma(V_0)}{M}t$, $\tau = \frac{|V_0|M}{F}$, and V_0 is the velocity after a collision, which is given by

$$V_0 = \frac{(1+\alpha_+)v}{1+\mu} \quad \text{for} \quad v > 0 \tag{18}$$

and

$$V_0 = \frac{(1+\alpha_-)v}{1+\mu} \quad \text{for} \quad v < 0. \tag{19}$$

Integrating over time, one obtains

$$\langle V \rangle = \frac{M\rho[(1+\alpha_+)^2 - (1+\alpha_-)^2]}{2F(1+\mu)^2}\int_0^{\infty} dv\, v^3 \phi(v), \tag{20}$$

where we have assumed that $\phi(v)$ is symmetric. With this assumption the sign of the motor effect is independent of the form of the bath velocity distribution. For a Gaussian bath distribution, the dimensionless mean velocity $\langle V^* \rangle$ is given explicitly by

$$\langle V^* \rangle = \frac{[(1+\alpha_+)^2 - (1+\alpha_-)^2]\mu}{2F^*(1+\mu)^2}\sqrt{\frac{2}{\pi}}. \tag{21}$$

A second quantity of interest is the integral of the velocity distribution

$$I_f = \rho \int_{-\infty}^{\infty} dv|v|\phi(v)\tau = \frac{\rho(2+\alpha_+ +\alpha_-)M}{F(1+\mu)} \int_0^{\infty} dv\, v^2\phi(v). \quad (22)$$

For a Gaussian bath distribution, one has

$$I_f = \frac{(2+\alpha_+ +\alpha_-)\mu}{2F^*(1+\mu)}. \quad (23)$$

This quantity corresponds to the value of γ in the limit of large friction (or small ratio τ_s/τ_c). Figure 5 shows the $\delta(V^*)$ contribution to $f(V^*)$, $1-\gamma$, for two mass ratios $M/m = 10,20$. The full curves correspond to the simulation of the Boltzmann-Lorentz equation. The expression of the kick model Eq. (23) (dotted curves) gives the correct asymptotic behavior for large friction, but underestimates the $\delta(V^*)$ contribution to $f(V^*)$ at low friction. By using the exact expression Eq. (16), where C is obtained from an exact asymptotic expansion of Eq. (22) and matching with the independent kick model Eq. (16), one obtains a very accurate description for all friction (dot-dashed curves). The remaining small excess is due to the fact C is set to a constant, but in reality depends slightly on F^*.

The characteristic function can also be calculated:

$$\langle e^{ikV}\rangle = \rho \int_{-\infty}^{\infty} dv|v|\phi(v) \int_0^{\tau} e^{ikV(t)}dt. \quad (24)$$

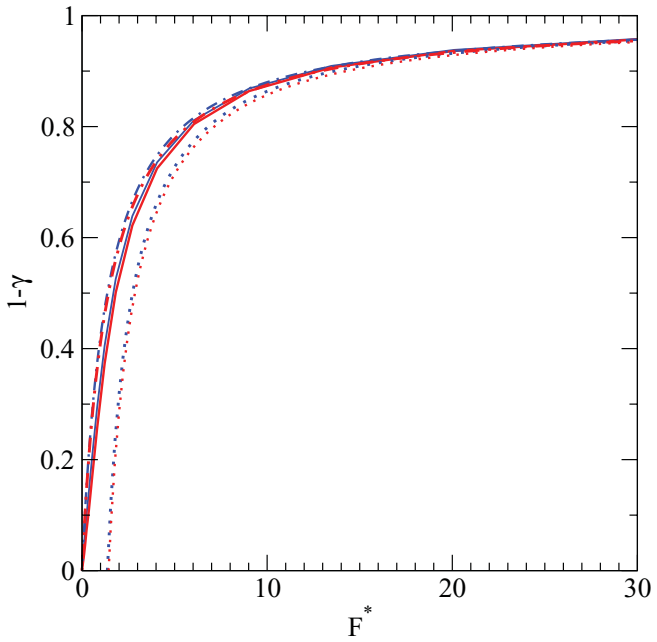

FIG. 5. (Color online) $\delta(V^*)$ contribution to $f(V^*)$, $1-\gamma$, of an asymmetric granular piston versus F^* with $\alpha_+ = 1$ and $\alpha_- = 0$, for $\mu = 10,20$. The full curves show the simulation results. The dotted curves correspond to the analytical expression of the kick model, and the dot-dashed curves to Eq. (16) where C is calculated from the exact expression in the high friction limit.

Integrating over time, one obtains

$$\langle e^{ikV}\rangle = \frac{M\rho}{ikF} \int_0^{\infty} dv\, v\phi(v) \times \left[\exp\left(\frac{ik(1+\alpha_+)v}{1+\mu}\right) - \exp\left(\frac{-ik(1+\alpha_-)v}{1+\mu}\right)\right]. \quad (25)$$

Taking the inverse Fourier transform, one infers the velocity distribution $f_R(V)$:

$$\gamma f_R(V) = \frac{M\rho}{F}\left[\theta(V)\int_{\frac{(1+\mu)V}{1+\alpha_+}}^{\infty} dv|v|\phi(v) + \theta(-V)\int_{-\infty}^{\frac{(1+\mu)V}{1+\alpha_-}} dv|v|\phi(v)\right]. \quad (26)$$

Note that the regular velocity distribution $f_R(V)$ is continuous at $V = 0$. For a Gaussian bath distribution, the dimensionless velocity distribution is then given by

$$\gamma f_R(V^*) = \frac{\mu}{F^*}\sqrt{\frac{1}{2\pi}}\left[\theta(V^*)\exp\left(-\frac{(1+\mu)^2V^{*2}}{2(1+\alpha_+)^2}\right) + \theta(-V^*)\exp\left(-\frac{(1+\mu)^2V^{*2}}{2(1+\alpha_-)^2}\right)\right]. \quad (27)$$

Velocity distributions are displayed in Fig. 6 for different values of the solid friction. As expected, the amplitude decreases as this quantity increases. Rescaled distributions $F^*\gamma f_R(V^*)$ versus V^* are shown in Fig. 7, where one observes that for $F^* > 2$, curves converge toward the exact result, Eq. (27).

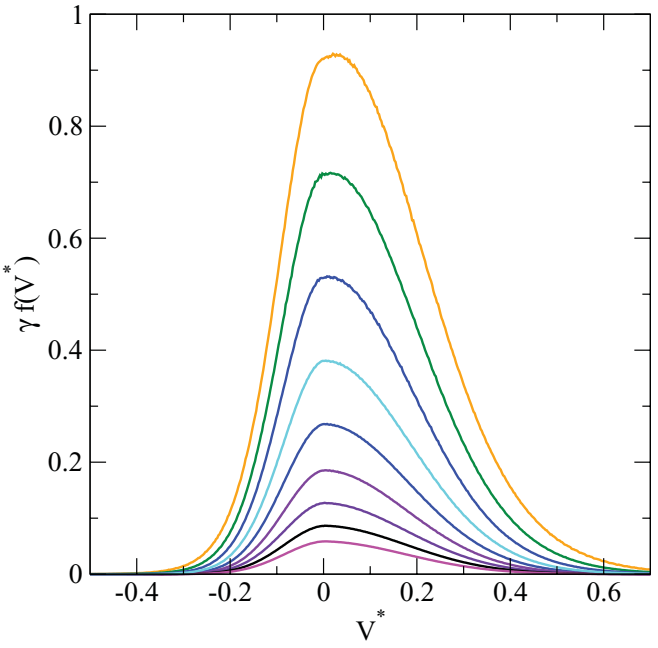

FIG. 6. (Color online) Dimensionless velocity distributions $\gamma f(V^*)$ from simulation for various dimensionless friction forces $F^* = 2.72,6.05,6.6,9.02,13,6,20.09,30.0,44.7,66.7$ (from top to bottom).

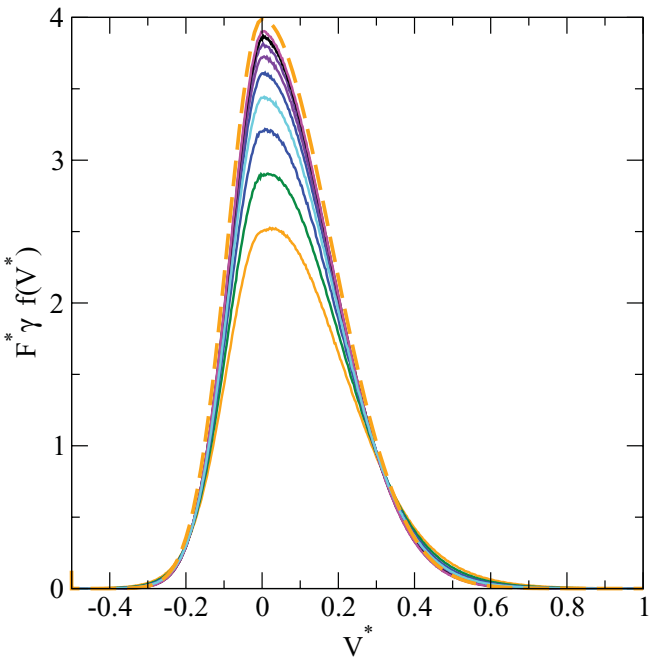

FIG. 7. (Color online) Rescaled velocity distributions $F^*\gamma f(V^*)$ for the same values of F^* as in Fig. 6 but in reverse order. The dashed curve shows the prediction of the independent kick model, Eq. (27).

VI. THE BROWNIAN LIMIT AND THE FOKKER-PLANCK EQUATION

We now consider the opposite limit when the stopping time τ_s is much larger than the mean time between bath collisions, τ_c. For homogeneous granular motors where the mean velocity goes to zero in the Brownian limit [18,48], a standard Kramers-Moyal expansion of the BL integral operator leads to the Fokker-Planck differential operator. For heterogeneous granular motors, where the mean velocity remains finite and independent of the mass ratio in the Brownian limit, some caution is needed: The perturbative expansion must be performed around the nonzero mean velocity (rather than around zero) [49]. Finite mass corrections, however, cannot be easily included.

The approach we proposed in Ref. [37] consists of reexpressing the BL operator as a complete series expansion in terms of the derivatives of the velocity distribution function. Applying the same method to the piston we have, e.g.,

$$f\left(V-\frac{1+\alpha_+}{1+\mu}y\right)=\sum_{n=0}^{\infty}\left(\frac{1+\alpha_+}{1+\mu}\right)^n\frac{(-y)^n}{n!}\frac{\partial^n f(V)}{\partial V^n}, \tag{28}$$

with similar expressions for $\phi(V+y-\frac{1+\alpha_+}{1+\mu}y)$, $f(V+\frac{1+\alpha_-}{1+\mu}y)$, and $\phi(V-y+\frac{1+\alpha_-}{1+\mu}y)$. Inserting these in the BL equation (8) allows us to write the collision operator as

$$J[f,\phi]=\sum_{n=1}^{\infty}\frac{1}{n!\mu^n}\frac{\partial^n[g_n(V)f(V)]}{\partial V^n}, \tag{29}$$

where we have used the fact that the zero-order terms of the expansion cancel the destruction term and where we have introduced

$$g_n(V)=\rho\int_0^{\infty}dy\,y^{n+1}\left[\left(-\mu\frac{1+\alpha_+}{1+\mu}\right)^n\phi(V+y)+\left(\mu\frac{1+\alpha_-}{1+\mu}\right)^n\phi(V-y)\right] \tag{30}$$

The functions $g_n(V)$ can be obtained from the generating function

$$g(V,a)=\rho\int_0^{\infty}dy\,y\left[\exp\left(\frac{-(1+\alpha_+)\mu ya}{1+\mu}\right)\phi(V+y)+\exp\left(\frac{(1+\alpha_-)\mu ya}{1+\mu}\right)\phi(V-y)\right] \tag{31}$$

Truncating the BL operator Eq. (29) at second order and adding the dry friction leads to the following Fokker-Planck equation:

$$\frac{\partial f(V,t)}{\partial t}=\frac{1}{M}\frac{\partial}{\partial V}\{[F\sigma(V)+mg_1(V)]f(V,t)\}+\frac{1}{2M^2}\frac{\partial^2}{\partial V^2}[m^2g_2(V)f(V,t)], \tag{32}$$

in which all finite-mass corrections are incorporated, and where deviations from a Gaussian distribution are present for large finite masses. Recalling that the $g_n(V)$ are proportional to ρ, we see that for a given dry friction F increasing the bath density reduces the effect of friction. The corresponding Langevin equation [50] features a motor force with a nonlinear dependence on V and an additive noise:

$$M\frac{dV}{dt}=-F\sigma(V)-mg_1(V)+m\sqrt{g_2(V)}\eta(t), \tag{33}$$

where $\eta(t)$ is a white Gaussian noise with $\langle\eta(t)\rangle=0$ and $\langle\eta(t)\eta(t')\rangle=\delta(t-t')$.

The steady-state solution of Eq. (32) is

$$f(V)=\frac{C_f}{g_2(V)}\exp\left[-2M\int_0^V du\,\left(\frac{mg_1(u)+F\sigma(u)}{m^2g_2(u)}\right)\right], \tag{34}$$

where C_f is obtained from the normalization condition $\int dVf(V)=1$. This result clearly shows that, even in the absence of friction, the velocity distribution is non-Gaussian for finite mass ratios.

In the Brownian limit $g_1(V)\sim g_1'(\tilde{V})(V-\tilde{V})$ and $g_2(V)=2T_g/mg_1'(\tilde{V})$, where T_g (the granular temperature of the piston, which is lower than the bath temperature T) and $\tilde{V}$ are given by the Kramers-Moyal expansion [Eqs. (6) and (8) in Ref. [11]]. (Physically, $\tilde{V}$ is the exact steady-state drift velocity of a piston in the Brownian limit in the absence of friction.) This finally gives a stationary distribution, at the lowest order in m/M,

$$f(V)=C\exp\left(-\frac{M(V-\tilde{V})^2}{2T_g}-\frac{\mu F|V|}{g_1'(\tilde{V})T_g}\right), \tag{35}$$

where C is the normalization constant. Whereas one observes a Gaussian decay of the velocity distribution at large velocity, $f(V)$ decreases exponentially for small and intermediate velocities due to friction [22,29,32].

VII. STATIC FRICTION

Our analysis has so far been restricted to dynamic dry friction that produces a constant retarding force on a moving piston. A stationary piston acquires a nonzero velocity following a collision with a bath particle, no matter how slowly the latter is moving. In reality, static friction will also be present and this will prevent the piston from moving unless it is struck by a sufficiently fast-moving bath particle. To model this effect correctly using a coefficient of static friction we would need to know the time-dependent force acting on a stationary piston during a collision with a bath particle. If this force exceeds the force due to static friction, the piston starts to move. In the present model, however, the collisions are assumed to be instantaneous. When a bath particle collides with a stationary piston it exerts on it an impulse $I = -(mv' - mv)$. We represent static friction in an approximate way, by introducing a threshold impulse I_m so that the piston is set into motion only if $|I| > I_m$.

The collision equation can be written as

$$I = -(mv' - mv) = MV' + I_s, \tag{36}$$

where I_s, which accounts for the loss of momentum due to friction, is given by

$$I_s = \begin{cases} I & \text{if} \quad |I| < I_m, \\ \sigma(v) I_m & \text{if} \quad |I| > I_m. \end{cases} \tag{37}$$

Introducing the definition of the coefficient of restitution, $v' - V' = -\alpha_\pm v$, we obtain that

$$V' = \begin{cases} \frac{m}{m+M}(1+\alpha_+)v - \frac{I_m}{m+M} & \text{if} \quad v > \frac{I_m}{m(1+\alpha_+)}, \\ \frac{m}{m+M}(1+\alpha_-)v + \frac{I_m}{m+M} & \text{if} \quad v < -\frac{I_m}{m(1+\alpha_-)}, \\ 0 & \text{otherwise.} \end{cases} \tag{38}$$

Therefore a bath particle moving with a velocity in the range $v_m^- < v < v_m^+$ where

$$v_m^\pm = \pm \frac{I_m}{m(1+\alpha_\pm)} \tag{39}$$

does not exert sufficient impulse and the piston remains at rest after a collision. Note that the threshold velocity decreases as the coefficient of restitution increases. The energy change is

$$\Delta E = \begin{cases} -\frac{1}{2} m v^2 (1 - \alpha_\pm^2), & |I| < I_m, \\ \frac{-mM(1-\alpha_\pm^2)v^2 - 2m|v|I_m + I_m^2}{2(m+M)}, & |I| > I_m. \end{cases} \tag{40}$$

We note that, because of the inclusion of static friction, $\Delta E \neq 0$ for $\alpha_\pm = 1$ (when $I > I_m$) as part of the impulse is used to do work against the static friction.

When the time scale ratio $\tau_s/\tau_c \gg 1$, it is easy to generalize the independent kick model by adding the static friction. The drift velocity is given by

$$\langle V \rangle = \rho \int_{v_m^+}^{\infty} dv\, v \phi(v) \int_0^\tau dt\, V(t) + \rho \int_{-\infty}^{v_m^-} dv |v| \phi(v) \int_0^\tau dt\, V(t), \tag{41}$$

where $V(t) = V_0 - \frac{F\sigma(V)}{M} t$, $\tau = \frac{M|V_0|}{F}$, and V_0 is given by Eq. (38).

Integrating over time, one obtains the following expression:

$$\langle V \rangle = \frac{M\rho}{2F(1+\mu)^2} \left((1+\alpha_+)^2 \int_{v_m^+}^{\infty} dv\, v (v - v_m^+)^2 \phi(v) - (1+\alpha_-)^2 \int_{-\infty}^{v_m^-} dv\, |v| (v_m^- - v)^2 \phi(v) \right). \tag{42}$$

Let us introduce the dimensionless threshold impulse

$$I_m^* = \frac{I_m}{\sqrt{mT}}. \tag{43}$$

Then for a Gaussian bath velocity distribution the dimensionless mean velocity is given by

$$\langle V^* \rangle = \frac{\mu}{2F^*(1+\mu)^2} [h(I_m^*, \alpha_+) - h(I_m^*, \alpha_-)] \tag{44}$$

with

$$h(I_m^*, \alpha) = (1+\alpha)^2 \sqrt{\frac{2}{\pi}} \exp\left(-\frac{I_m^{*2}}{2(1+\alpha)^2} \right) - (1+\alpha) I_m^* \operatorname{erfc}\left(\frac{I_m^*}{\sqrt{2}(1+\alpha)} \right) \tag{45}$$

that correctly reduces to Eq. (21) if $I_m^* = 0$. Figure 8 shows that the theoretical result is in good agreement with numerical simulations of the Boltzmann-Lorentz equation with static and dynamic friction.

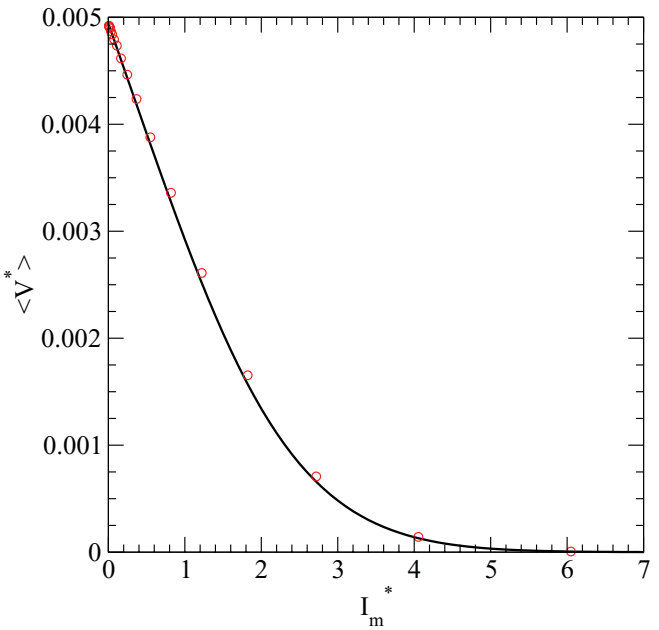

FIG. 8. (Color online) Dimensionless mean velocity of an asymmetric granular piston of mass ratio $\mu = 10$ with a friction force $F^* = 20.01$ with $\alpha_+ = 1$ and $\alpha_- = 0$, versus the threshold impulse. The circles correspond to the simulation results with the static friction and the solid lines show the theoretical result Eq. (44).

Developing Eq. (44) as a power series about $I_m^* = 0$, we obtain

$$\langle V^* \rangle = \frac{\mu}{2F^*(1+\mu)^2}(\alpha_+ - \alpha_-) \times \left[(2+\alpha_+ + \alpha_-)\sqrt{\frac{2}{\pi}} - I_m^* + O\left(I_m^{*4}\right) \right]. \quad (46)$$

We note the absence of terms in I_m^{*2} and I_m^{*3} and from Fig. 8 we see that the mean velocity increases linearly for $I_m^* < 2$. Furthermore, a nonzero impulse threshold means that, in addition to the simple scaling behavior ($\langle V \rangle \sim T^{3/2}$) with only dynamic friction present, a subdominant term appears:

$$\langle V \rangle \propto (\alpha_+ - \alpha_-)\left[(2+\alpha_+ + \alpha_-)\sqrt{\frac{2}{\pi}} T^{3/2} - \frac{I_m}{\sqrt{m}} T \right]. \quad (47)$$

The asymptotic behavior for large values of I_m^* is

$$\langle V^* \rangle = \frac{\mu}{2F^*(1+\mu)^2} \frac{1}{I_m^{*2}} \sqrt{\frac{2}{\pi}} \left[(1+\alpha_+)^4 \exp \times \exp\left(-\frac{I_m^{*2}}{2(1+\alpha_+)^2} \right) - (1+\alpha_-)^4 \times \exp\left(-\frac{I_m^{*2}}{2(1+\alpha_-)^2} \right) \right]. \quad (48)$$

In this limit only fast-moving bath particles, which are few since they correspond to the tails of the bath velocity distribution, can actuate a stationary piston. Therefore, the motor effect vanishes. The integral of the velocity distribution is

$$I_f = \frac{M\rho}{(1+\mu)F} \left[(1+\alpha_+) \int_{v_m^+}^{\infty} dv\, v(v - v_m^+)\phi(v) + (1+\alpha_-) \int_{-\infty}^{v_m^-} dv |v| (v_m^- - v)\phi(v) \right], \quad (49)$$

which, for a Gaussian bath velocity distribution, gives

$$I_f = \frac{\mu}{2(1+\mu)F^*} \left[(1+\alpha_+)\mathrm{erfc}\left(\frac{I_m^*}{\sqrt{2}(1+\alpha_+)} \right) + (1+\alpha_-)\mathrm{erfc}\left(\frac{I_m^*}{\sqrt{2}(1+\alpha_-)} \right) \right]. \quad (50)$$

This goes rapidly to zero for $I_m^* > 2$.

Finally, the characteristic function $\langle e^{ikV} \rangle$ is given by

$$\langle e^{ikV} \rangle = \frac{\rho M}{F} \left[\int_{v_m^+}^{\infty} dv |v| \phi(v) \frac{e^{i[(1+\alpha_+)/(1+\mu)]k(v - v_m^+)} - 1}{ik} - \int_{-\infty}^{v_m^-} dv |v| \phi(v) \frac{e^{i[(1+\alpha_-)/(1+\mu)]k(v - v_m^-)} - 1}{ik} \right]. \quad (51)$$

Taking the inverse Fourier transform, one obtains the velocity distribution

$$\gamma f_R(V) = \frac{\rho M}{F} \left[\theta(V) \int_{v_m^+ + \frac{1+\mu}{1+\alpha_+}V}^{\infty} dv |v| \phi(v) + \theta(-V) \int_{-\infty}^{v_m^- + \frac{1+\mu}{1+\alpha_-}V} dv |v| \phi(v) \right]. \quad (52)$$

For a Gaussian distribution, the dimensionless velocity distribution is expressed as

$$\gamma f_R(V^*) = \frac{\mu}{F^*} \sqrt{\frac{1}{2\pi}} \left[\theta(V^*) \exp\left(-\frac{[I_m^* + (1+\mu)V^*]^2}{2(1+\alpha_+)^2} \right) + \theta(-V^*) \exp\left(-\frac{[-I_m^* + (1+\mu)V^*]^2}{2(1+\alpha_-)^2} \right) \right]. \quad (53)$$

We see that static friction has a dramatic qualitative effect on the regular velocity distribution in the sense that it is discontinuous at $V^* = 0$, a feature not present for $I_m^* = 0$:

$$\gamma f_R(0+) - \gamma f_R(0-) = \frac{\mu}{F^*} \sqrt{\frac{1}{2\pi}} \left[\exp\left(-\frac{I_m^{*2}}{2(1+\alpha_+)^2} \right) - \exp\left(-\frac{I_m^{*2}}{2(1+\alpha_-)^2} \right) \right]. \quad (54)$$

Figure 9 shows velocity distributions obtained from simulations of the Boltzmann-Lorentz equation with static and

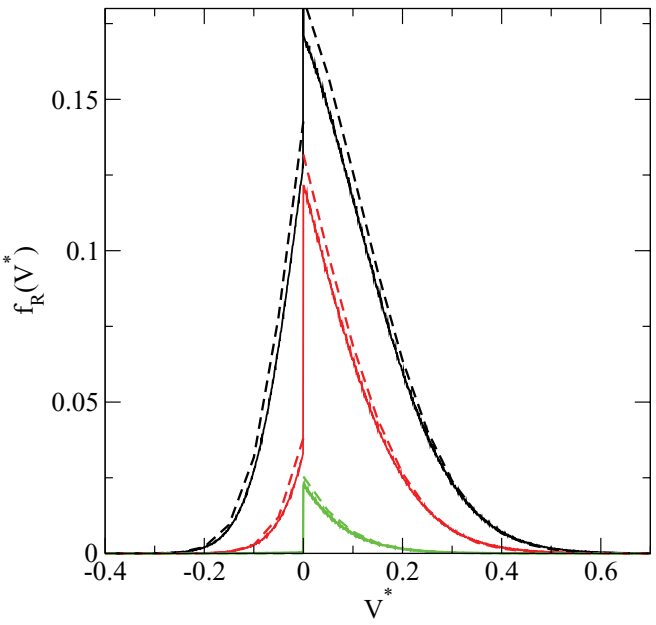

FIG. 9. (Color online) Dimensionless velocity distributions of an asymmetric granular piston of mass ratio $\mu = 10$ a friction force for $\alpha_+ = 1$ and $\alpha_- = 0$, with different impulse threshold $I_m^* = 0.82, 1.82, 4.06$, top to bottom. The dashed curves correspond to the analytical expression of the independent kick model with the static and dynamic frictions, Eq. (53), and the full curves show the simulation results of the Boltzmann-Lorentz equation.

dynamic friction when $F^* = 20.01$, $\mu = 10$, and for different values of the impulse threshold (full curves). The independent kick model incorporating dynamic and static friction provides an accurate description of the kinetic properties of the Boltzmann-Lorentz equation. As expected, one observes a finite discontinuity of the velocity distribution at $V = 0$. Negative piston velocities occur less frequently than positive ones due to the low efficiency of bath collisions on the right side of the piston ($\alpha_- = 0$) and the momentum threshold of the static friction. As the static friction increases, motion of the piston to the left is reduced more rapidly than motion to the right.

VIII. CONCLUSION

We have considered the effect of dynamic and static friction on the kinetics of a granular asymmetric piston. When only dynamic friction is present, the mean velocity exhibits two scaling regimes depending on the strength of the friction force. In the high friction limit, the Boltzmann-Lorentz equation is asymptotically described by a solvable independent kick model. Conversely, when the friction is small, and if the mass ratio is large, the model can be mapped to Fokker-Planck equation, for which exact results can be also obtained. When static, as well as dynamic, friction is present the mean piston velocity initially decreases linearly with the threshold impulse, while for larger values of this parameter the motor effect is rapidly suppressed, decreasing in a Gaussian fashion. Further investigation could consider collective effects of motor assemblies observed in biological systems [51–53] or dense granular systems with active particles [54–57].

ACKNOWLEDGMENTS

We thank a referee for suggesting that we derive the independent kick model from the Boltzmann-Lorentz equation.

APPENDIX: DERIVATION OF THE INDEPENDENT KICK MODEL FROM THE BOLTZMANN-LORENTZ EQUATION

For the sake of simplicity, we consider here the Boltzmann-Lorentz model with dynamic friction only, but the method can be generalized to include static as well as dynamic friction and for other granular motors. In the large friction limit the velocity distribution, which is given by Eq. (14), corresponds to $\gamma \to 0$. In this regime, the dominant contribution of the collision integral of Eq. (8) is given by inserting the singular part of the velocity distribution, and the stationary Boltzmann-Lorentz equation can be expressed for $V \neq 0$ as

$$-\gamma \frac{F\sigma(V)}{M\rho}\frac{\partial}{\partial V} f_R(V) = (1-\gamma)\int_0^\infty dy\, y\left[\delta\left(V - \frac{1+\alpha_+}{1+\mu}y\right)\phi\left(V + \frac{\mu-\alpha_+}{1+\mu}y\right)\delta\left(V + \frac{1+\alpha_-}{1+\mu}y\right)\phi\left(V - \frac{\mu-\alpha_-}{1+\mu}y\right)\right]. \tag{A1}$$

Note that the loss term of the Boltzmann equation does not appear here, because it gives a singular contribution at $V = 0$ and a regular part proportional to γ, which is negligible in the large friction limit. By using the fact that $1 - \gamma \simeq 1$ and integrating the right hand side of Eq. (A1) over y, one obtains

$$-\gamma \frac{F\sigma(V)}{M\rho}\frac{\partial}{\partial V} f_R(V) = \theta(V)\left(\frac{1+\mu}{1+\alpha_+}\right)^2 V\phi\left[V\left(\frac{1+\mu}{1+\alpha_+}\right)\right] + \theta(-V)\left(\frac{1+\mu}{1+\alpha_-}\right)^2 V\phi\left[V\left(\frac{1+\mu}{1+\alpha_-}\right)\right]. \tag{A2}$$

Finally, by integrating Eq. (A2) from $V > 0$ to ∞ and from $-\infty$ to $V < 0$, and changing the variable $u = V(\frac{1+\mu}{1+\alpha_\pm})$, one recovers Eq. (26).

[1] H. B. Callen, *Thermodynamics* (John Wiley and Sons, New York, 1960).
[2] J. Piasecki and C. Gruber, Physica A **265**, 463 (1999).
[3] C. Gruber and J. Piasecki, Physica A **268**, 412 (1999).
[4] C. Gruber, S. Pache, and A. Lesne, J. Stat. Phys. **108**, 669 (2002).
[5] C. Gruber, S. Pache, and A. Lesne, J. Stat. Phys. **112**, 1177 (2003).
[6] C. Gruber and A. Lesne, in *Encyclopedia of Mathematical Physics*, edited by J.-P. Franoise, G. L. Naber, and T. S. Tsun (Academic Press, Oxford, 2006), p. 160.
[7] R. Brito, M. J. Renne, and C. V. den Broeck, Europhys. Lett. **70**, 29 (2005).
[8] J. J. Brey and N. Khalil, Phys. Rev. E **82**, 051301 (2010).
[9] G. Costantini, U. M. B. Marconi, and A. Puglisi, Phys. Rev. E **75**, 061124 (2007).
[10] G. Costantini, U. Marini Bettolo Marconi, and A. Puglisi, Europhys. Lett. **82**, 50008 (2008).
[11] J. Talbot, A. Burdeau, and P. Viot, Phys. Rev. E **82**, 011135 (2010).
[12] P. Eshuis, K. van der Weele, D. Lohse, and D. van der Meer, Phys. Rev. Lett. **104**, 248001 (2010).
[13] M. Smoluchowski, Phys. Z. **13**, 1069 (1912).
[14] R. P. Feynman, R. B. Leighton, and M. L. Sands, *The Feynman Lectures on Physics* (Addison-Wesley, Reading, MA, 1963).
[15] P. Reimann, Phys. Rep. **361**, 57 (2002).
[16] F. Jülicher, A. Ajdari, and J. Prost, Rev. Mod. Phys. **69**, 1269 (1997).
[17] M. van den Broek, R. Eichhorn, and C. Van den Broeck, Europhys. Lett. **86**, 30002 (2009).

[18] B. Cleuren and C. V. den Broeck, Europhys. Lett. **77**, 50003 (2007).
[19] B. Cleuren and R. Eichhorn, J. Stat. Mech. (2008) P10011.
[20] G. Costantini, A. Puglisi, and U. Marconi, Eur. Phys. J. Spec. Top. **179**, 197 (2009).
[21] S. Daniel, M. K. Chaudhury, and P.-G. de Gennes, Langmuir **21**, 4240 (2005).
[22] M. K. Chaudhury and S. Mettu, Langmuir **24**, 6128 (2008).
[23] P. S. Goohpattader, S. Mettu, and M. K. Chaudhury, Langmuir **25**, 9969 (2009).
[24] P. Goohpattader, S. Mettu, and M. Chaudhury, Eur. Phys. J. E **34**, 1 (2011).
[25] T. K. Caughey and J. K. Dienes, J. Appl. Phys. **32**, 2476 (1961).
[26] J. Atkinson and T. Caughey, Int. J. Non-Linear Mech. **3**, 399 (1968).
[27] P. G. de Gennes, J. Stat. Phys. **119**, 953 (2005).
[28] H. Hayakawa, Physica D **205**, 48 (2005).
[29] A. Kawarada and H. Hayakawa, J. Phys. Soc. Jpn. **73**, 2037 (2004).
[30] A. M. Menzel and N. Goldenfeld, Phys. Rev. E **84**, 011122 (2011).
[31] A. Mauger, Physica A **367**, 129 (2006).
[32] H. Touchette, E. V. der Straeten, and W. Just, J. Phys. A **43**, 445002 (2010).
[33] A. Baule, E. G. D. Cohen, and H. Touchette, J. Phys. A **43**, 025003 (2010).
[34] A. Baule, H. Touchette, and E. G. D. Cohen, Nonlinearity **24**, 351 (2011).
[35] A. Buguin, F. Brochard, and P.-G. de Gennes, Eur. Phys. J. E **19**, 31 (2006).
[36] S. Mettu and M. K. Chaudhury, Langmuir **26**, 8131 (2010).
[37] J. Talbot, R. D. Wildman, and P. Viot, Phys. Rev. Lett. **107**, 138001 (2011).
[38] R. D. Wildman, J. M. Huntley, and D. J. Parker, Phys. Rev. E **63**, 061311 (2001).
[39] J. Talbot and P. Viot, Phys. Rev. Lett. **89**, 064301 (2002).
[40] G. W. Baxter and J. S. Olafsen, Nature (London) **425**, 680 (2003).
[41] A. Burdeau and P. Viot, Phys. Rev. E **79**, 061306 (2009).
[42] J. Piasecki, J. Talbot, and P. Viot, Phys. Rev. E **75**, 051307 (2007).
[43] J. Talbot and P. Viot, J. Phys. A **39**, 10947 (2006).
[44] G. Bird, *Molecular Gas Dynamics and the Direct Simulation of Gas Flows* (Clarendon Press, Oxford, 1994).
[45] J. J. Brey, M. J. Ruiz-Montero, and D. Cubero, Phys. Rev. E **54**, 3664 (1996).
[46] J. M. Montanero and A. Santos, Granular Matter **2**, 53 (2000).
[47] J. M. Montanero, V. Garzo, A. Santos, and J. Brey, J. Fluid Mech. **389**, 391 (1999).
[48] J. J. Brey, J. W. Dufty, and A. Santos, J. Stat. Phys. **97**, 281 (1999).
[49] J. Talbot, A. Burdeau, and P. Viot, J. Stat. Mech. (2011) P03009.
[50] C. W. Gardiner, *Stochastic Methods: A Handbook for the Natural and Social Sciences* (Springer, Berlin, 2009).
[51] J. Howard, Annu. Rev. Biophys. **38**, 217 (2009).
[52] T. Guérin, J. Prost, and J.-F. Joanny, Phys. Rev. Lett. **104**, 248102 (2010).
[53] T. Guérin, J. Prost, and J.-F. Joanny, Phys. Rev. Lett. **106**, 068101 (2011).
[54] S. Mishra, A. Baskaran, and M. C. Marchetti, Phys. Rev. E **81**, 061916 (2010).
[55] A. Baskaran and M. C. Marchetti, Phys. Rev. Lett. **101**, 268101 (2008).
[56] J. Deseigne, O. Dauchot, and H. Chaté, Phys. Rev. Lett. **105**, 098001 (2010).
[57] A. Baskaran and M. C. Marchetti, J. Stat. Mech. (2011) P04019.